

Inside this issue:

(4 pages)

Kelvin-Helmholtz instability in Rotating Shear flows: The Role of Coriolis Force 1

Profiling HPC Application using NVIDIA Nsight Systems 3

ANTYA Usage Statistics and Observed workloads - Feb 2025 4



Kelvin-Helmholtz instability in Rotating Shear flows: The Role of Coriolis Force

Prince Kumar (PDF, Basic Theory and Simulation Division, IPR)

Email: prince.kumar@ipr.res.in

Rotating fluids are fundamental in geophysical and astrophysical systems, where forces such as the Coriolis and centrifugal forces influence large-scale flow dynamics and the onset of instabilities [1-3].

These instabilities facilitate momentum and energy transport, impacting atmospheric circulation, ocean currents, and the evolution of astrophysical objects [2,3]. The Kelvin-Helmholtz Instability (KHI) arises in shear flows with velocity discontinuities between fluid layers and is commonly observed in planetary atmospheres, oceanic flows, and astrophysical jets [2,3]. The growth and evolution of KHI are governed by various parameters, including surface tension, density stratification, gravity, magnetic fields, and rotation [2]. A magnetic field aligned with the shear flow suppresses the instability due to the Lorentz force, whereas a transverse magnetic field has a negligible effect [4]. Experimental evidence suggests that, in a rotating frame, fluid elements experience deflections due to the Coriolis force, equivalent to those induced by a magnetic field [5]. The Coriolis force, acting perpendicular to the velocity field, constrains the KH vortex formation and turbulence evolution, similar to the role of the Lorentz force in magnetized plasmas [4,6]. This study investigates the influence of the Coriolis force on the KHI and its equivalence to the effects of a magnetic field. Using the beta-plane approximation, we analyse the stability of a two-dimensional shear flow under differential rotation. The evolution of an incompressible 2D fluid flow in a rotating frame is governed by the Euler equations, which consist of the mass conservation equation. To simplify the analysis, the vorticity stream function formulation is used, where the vorticity equation is given as [6],

$$\frac{\partial \omega_z}{\partial t} + (u \cdot \nabla) \omega_z = \nabla \times (2u \times \Omega) + \nu \nabla^2 \omega_z, \text{ and } \nabla^2 \psi = -\omega_z.$$

Under the beta-plane approximation, the above equation reduces to a simpler form which is given as,

$$\frac{\partial \omega_z}{\partial t} + J[\psi, \omega_z] - \beta \frac{\partial \psi}{\partial x} = \nu \nabla^2 \omega_z, \text{ where } \beta = \frac{2\Omega}{\omega_R} \text{ ----- 1}$$

The parameter Ω represents the rotational frequency and β is the Coriolis parameter. We have the normalizing parameters: radius of a planet r_0 , wave frequency ω_R and wave velocity U_R , ensuring that the variable ω_z and Ψ have the units (U_R/r_0) and $U_R r_0$, respectively. The Jacobian is defined as $J[\psi, \omega_z] = \partial_x \psi \partial_y \omega_z - \partial_x \omega_z \partial_y \psi$. We consider a large scale 2D periodic system with initial vorticity profile give as [6],

$$\omega_z = \frac{\omega_0}{\cosh^2\left(\frac{y+Ly/4}{d}\right)} - \frac{\omega_0}{\cosh^2\left(\frac{y-Ly/4}{d}\right)} + \frac{\omega_0}{\cosh^2\left(\frac{y-3Ly/4}{d}\right)} - \frac{\omega_0}{\cosh^2\left(\frac{y+3Ly/4}{d}\right)}.$$

The simulations are performed on ANTYA HPC Cluster at Institute for Plasma Research (IPR) using in-house developed pseudo-spectra code. The code is serial and runs on a single core of an ANTYA HPC node. The spatial and temporal discretization is done using the k and t variable, respectively, and satisfy the Courant-Friedrichs-Lewy (CFL) condition. The Adam-bashforth method has been used for time-stepping. For all the results presented in the following numerical analysis, we choose a grid of size $N_x \times N_y = 256 \times 256$ and the time step value is $10^{-3} \omega_R^{-1}$ [6]. After checking the reliability of the code with the Kelvin-Helmholtz instability in the absence of rotation ($\Omega =$

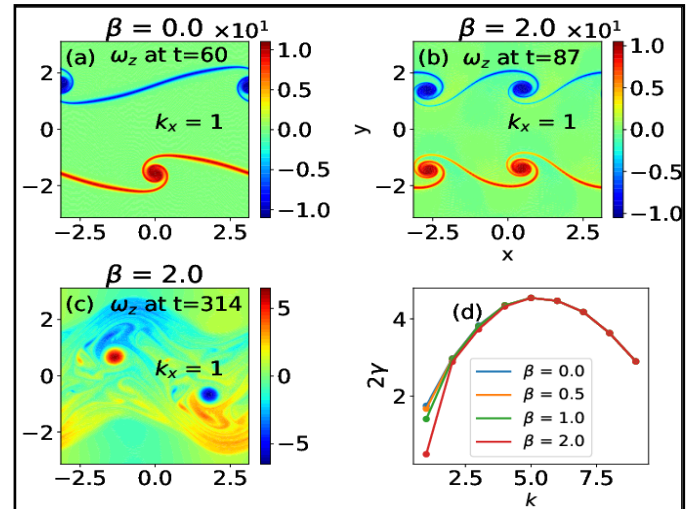


Fig (1): Figure (a) represents a snapshot of the time evolution of the imposed mode on $k_x = 1$ the initial vorticity profile ($\omega_0 = 12$) at $t = 69.08$ for $\beta = 0$. Figures (b) and (c) represent snapshots of its time evolution with $\beta = 2.0$ at different times, $t = 87.92$ and $t = 314$, respectively. Figure (d) represents the growth rate of different wavelengths or modes for various values of β . We fix the parameter $d = 0.078$

0), we focus on investigating the stability characteristics of the KH flow in the presence of finite rotation. In order to analyse the effect of finite rotation on the KH flow, we impose a perturbation on the initial vorticity profile at $t=0$, given by $A \cos(k_x x)$ where A is the amplitude, and k_x is the wave number along the x -direction. Figure 1 shows the time evolution of the perturbation in the $k_x = 1$ mode of the KH flow under rotation, quantified by the β parameter. The description of the other parameters involved is provided in the caption of the figure. The results presented here correspond to a shear flow vorticity strength, defined by $\omega_0 = 12$. The appearance of two vortex structures in Fig. 1 (b) suggests energy redistribution from the initial perturbed mode $k_x = 1$ to the second mode, $k_x = 2$. Energy initially cascades from $k_x = 1$ to $k_x = 2$, grows, and merges into a single vortex, as shown in Fig. 1(c). The growth rate of modes, shown in Fig. 1(d), remains unchanged for all β values, except for $k_x = 1$. This supports the analytical results [6,7], indicating that sheared flow velocity is unaffected by rotation until a high β is reached. In order to better understand the influence of the β on the instability, it is necessary to investigate scenarios with lower vorticity strength and higher β values.

We, therefore, examine the KH vortices under relatively lower shear flow vorticity ($\omega_0 = 2.0$) and higher β values. Figs. 2(a) and (b) show the snapshot of the vorticity profiles with $\beta = 0.0$, and $\beta = 0.5$, respectively, for perturbation mode $k_x = 1$ and initial flow velocity $U_0 = 0.15$ (relatively weaker than the previous case). The formation of two vortex structures in Fig. 2(b) again indicates energy redistribution from mode $k_x = 1$ to $k_x = 2$. Figs. 2(c) and (d) show the vorticity profiles for $\beta = 0.0$ and $\beta = 1.5$, respectively, for perturbation mode $k_x = 2$. In Fig. 2(d), four vortices form, showing the energy redistribution from mode $k_x = 2$ to $k_x = 4$.

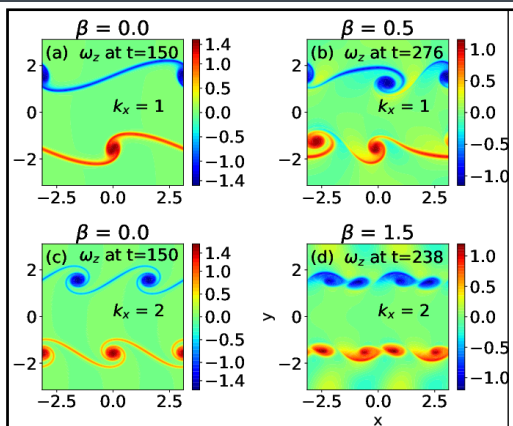


Fig (2): Figures (a) and (b) represent a snapshot of the time evolution of the imposed mode $k_x = 1$ on the initial vorticity profile ($\omega_0 = 2.0$) for $\beta = 0.0$ and 0.5 , respectively. Figures (c) and (d) represent a snapshot of the time evolution of the imposed mode on $k_x = 2$ the initial vorticity profile ($\omega_0 = 2.0$) for $\beta = 0.0$ and 1.5 , respectively.

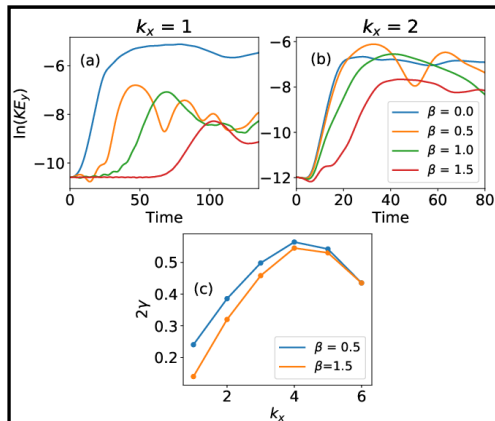


Fig (3): Figures (a) and (b) represent the time evolution logarithm of the kinetic energy along the y -direction for $k_x = 1$ and $k_x = 2$, respectively, with different values of β . Figure (c) represents the growth rate of different wavelengths or modes for different values of β .

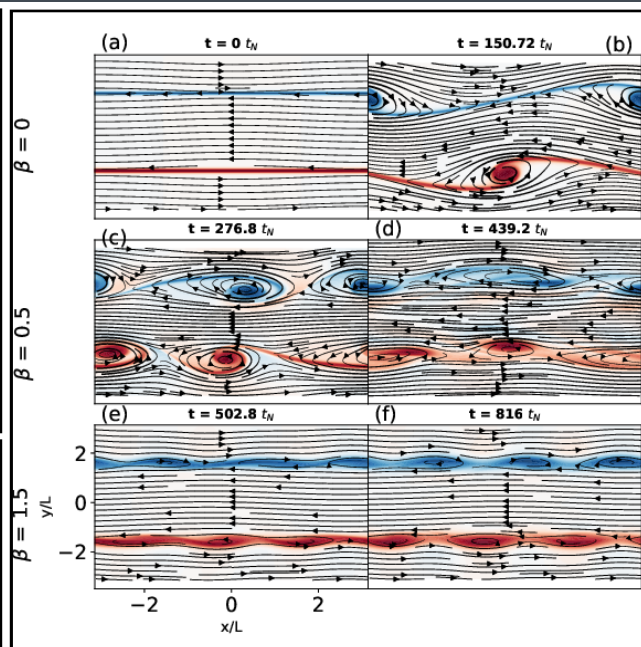


Fig (4): Snapshots of the streamline and vorticity of the sheared flow initially perturbed with mode $k_x = 1$ at different times $t = (\omega_R^{-1})$. Each row corresponds to a different value of the parameter β . Figures (a) and (b) are for $\beta = 0$, (c) and (d) are for $\beta = 0.5$, and (e) and (f) are for $\beta = 1.5$.

The growth rate profiles in Fig. 3 show significant changes even at $\beta = 0.5$, confirming that lower shear flow velocity profile is highly affected by rotation. The exponential growth of the perturbed vorticity in Fig. 3 demonstrates the instability growth and saturation in the nonlinear regime. The semi log plots in Figs. 3(a) and (b) for modes $k_x = 1$ and $k_x = 2$ show that as β increases, the mode growth decreases. Higher β values are required to affect higher modes for a fixed equilibrium flow velocity. These findings qualitatively align with theoretical predictions [6].

To gain a deeper understanding of these observations, we now examine, as shown in Fig. 4, the physical effects of rotation on the KH instability and draw analogies with the influence of magnetic fields. It has been predicted that a magnetic field parallel to the flow direction stabilizes the flow against small perturbations, with the Lorentz force contributing to this effect [4]. Similarly, the Coriolis force in a rotating frame mimics the Lorentz force [5]. The rotation force in the β -plane approximation acts eastward (x -direction), and the Coriolis effect directs the flow in the negative x -direction, assuming a positive β . In magnetized sheared flow, the Alfvén Mach number determines the stability of the KH flows [4], while β governs the growth rate of the KH instability. Both parameters suppress the KH mode growth, but on different scales—Alfvén Mach number affects shorter wavelengths, while β influences longer wavelengths. Fig. 3(c) demonstrates that β affects smaller k -values, while higher modes remain unaffected. In magnetized KH flow, lower unstable modes persist even under high magnetic fields [4], whereas this unstable region vanishes with even a small β value.

Fig. 4 illustrates the impact of rotation on the KHI for mode $k_x = 1$. Initially, the sheared flow, perturbed with $k_x = 1$, forms a billow that grows and eventually merges into a single vortex in the absence of rotation (Fig. 4(b)), indicating fluid mixing. As rotation is introduced (Fig. 4(c) and (d), with $\beta = 0.5$), two vortices form, compressed and elongated in the x -direction due to the combined effects of rotation and mean flow, similar to behaviour in magnetized sheared flows [4]. However, two vortices do not appear in the presence of a magnetic field. When β increases to 1.5 (Fig. 4(e) and (f)), the vortices become even more compressed and elongated, suggesting a diminishing destabilizing effect of rotation. At $\beta = 2.5$ (not shown here), a vortex sheet forms, characterized by compressed, flat vortices confined to the shear flow—similar to the vortex sheet observed in magnetized flow [4]. This demonstrates that rotation in the shear flows can produce vortex behaviour similar to magnetic fields, though at different β values. The Coriolis parameter β affects the Kelvin-Helmholtz Instability (KHI) through the term $\beta \frac{\partial \psi}{\partial x}$, which represents the external rotation varying linearly along the y -direction. While the y -direction flow experiences the Coriolis force, the x -direction is unaffected since the Coriolis parameter only varies along the y -axis. Fig. 4 shows that the flow in the negative x -direction is largely insensitive to the Coriolis force, causing adjacent vortices to flatten, while flow in the positive x -direction allows vortex curvature. This study does not address the magnetic field effect. An interesting extension would be to explore scenarios involving both pseudo-magnetic effects from rotation and real magnetic field effects. A quantitative analysis of the Coriolis and Lorentz forces can be done in the future.

References:

- [1] K. Lambeck, The Earth's variable rotation: geophysical causes and consequences (Cambridge University Press, 2005)
- [2] S. Chandrasekhar, Hydrodynamic and hydromagnetic stability (Courier Corporation, 2013).
- [3] P. G. Drazin, Introduction to hydrodynamic stability, Vol. 32 (Cambridge university press, 2002).
- [4] Y. Liu, Z. Chen, H. Zhang, and Z. Lin, Physics of Fluids 30 (2018)
- [5] P. Kumar and D. Sharma, Physics of Plasmas 28, 083704 (2021).
- [6] P. Kumar, and D Sharma. "Study on Kelvin Helmholtz shear flows subjected to differential rotation." *arXiv preprint arXiv:2406.06256* (2024).
- [7] L. Engevik, Journal of Fluid Mechanics 499, 315 (2004)

Profiling HPC Application using NVIDIA Nsight Systems

NVIDIA Nsight Systems is a powerful performance analysis tool for developers working with GPU and CPU applications. It enables system-wide profiling to optimize execution efficiency, reduce bottlenecks, and improve performance. Nsight Systems is beneficial for HPC, AI, and real-time applications, integrating with CUDA, OpenMP, and MPI. HPC applications involve complex computations and large data transfers, where profiling helps identify bottlenecks, optimize kernel execution, and reduce unnecessary memory transfers.

A `.qdrep` file is generated which is a **Nsight Systems report file**, contains profiling data collected during an application run. This file can be opened using the **Nsight Systems GUI** to analyze performance metrics such as CPU and GPU utilization, memory transfers etc.

Load Cuda module to use NVIDIA Nsight system.

```
[user@visualization ~]$ module load cuda/11.1.0
```

```
[user@visualization ~]$ nsys --version
```

```
NVIDIA Nsight Systems version 2020.3.4.32-52657a0
```

To Profile precompiled GPU Code, user may try following.

```
[user@visualization ~]$ nsys profile -o lammps_report mpirun -np 4 lmp_gpu -sf gpu -pk gpu 2 -in in.nemd
```

```
Collecting data...
```

```
Processing events...
```

```
Capturing symbol files...
```

```
Creating final output files...
```

```
Processing [=====100%]
```

```
Saved report file to "/tmp/nsys-report-5512-2f23-2d88-5505.qdrep"
```

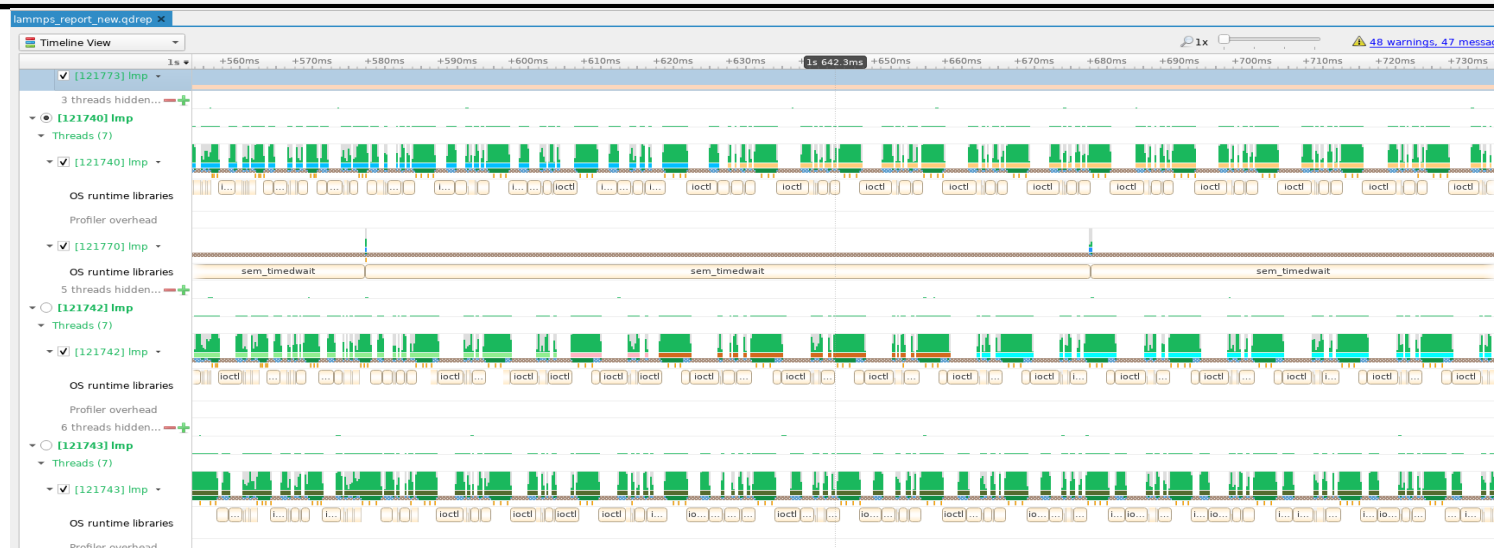
```
Report file moved to "/path/to/user/lammps_report.qdrep"
```

This will create a nsysms report file which is used in nsys-gui for analysing performance gaps.

To Open Nsight-GUI, user may try following command.

```
[user@visualization ~]$ nsys-ui
```

After Opening nsys-ui, open the qdrep(i.e. report) file which is generate after profiling from file->open menu.



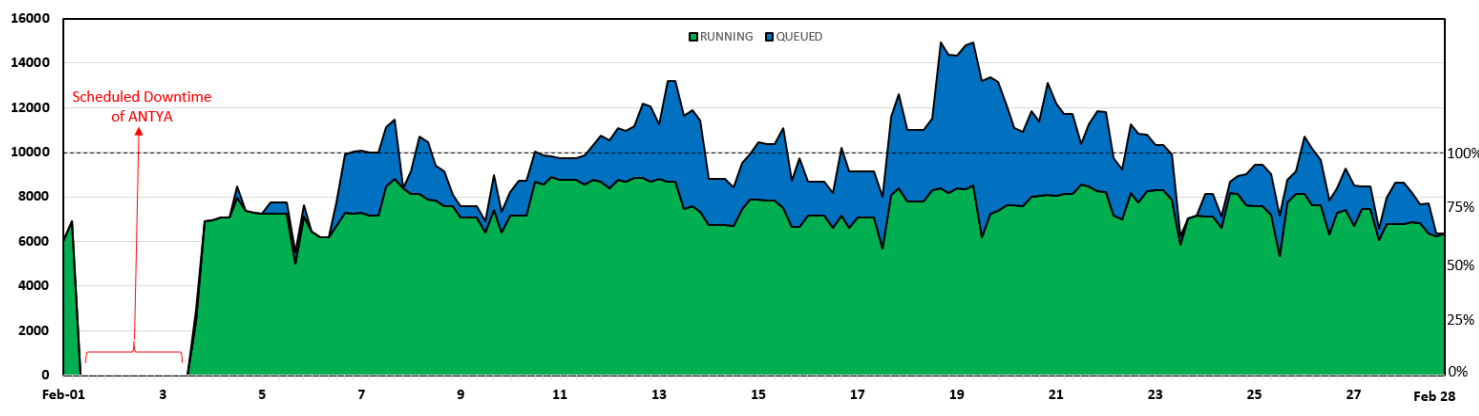
The LAMMPS code, compiled with CUDA, was profiled and analysed to evaluate its performance. The execution was conducted on four CPU cores, with two GPU cards handling the offloaded computations. The analysis revealed that for each CPU core offloaded to a GPU:

- The execution phase is represented in the green section of the profiling output.
- `ioctl` (Input/Output Control) is invoked to send commands to the GPU device driver via CUDA Driver APIs.
- `sem_timedwait` accounts for thread synchronization time.

These function calls belong to the operating system runtime library and contribute to execution overhead. Minimizing their impact can lead to improved performance and efficiency of the code.

ANTYA Utilization: February 2025

ANTYA DAILY OBSERVED WORKLOAD



ANTYA HPC Users' Statistics

February 2025

Total Successful Jobs~ 614

◆ Top Users (Cumulative Resources)

- CPU Cores **Amit Singh**
- GPU Cards **Abhishek Agraj**
- Walltime **Amit Singh**
- Jobs **Arzoo Malwal**

ANTYA Usage, Updates and News

- **Scheduled Downtime:** ANTYA underwent planned downtime from February 1 to February 3, 2025.
- **Job Submissions:** The highest job loads were observed in the *regularq*, *serialq*, *mediumq*, and *longq* queues, reflecting sustained user activity across multiple workloads in various queues.
- **Cluster Utilization:** The system maintained an average utilization of approximately 77%.
- **Packages/Applications Installed:** No New modules have been installed on ANTYA. To check list of available modules.
\$ module avail -l

Other Recent Work on HPC

Lower hybrid wave driven non thermal hard x-ray from ADITYA-U: Measurement and modelling study through synthetic diagnostics	Jagabandhu Kumar
Dynamics of unidirectional ELM current filaments and their merging	Nirmal K. Bisai
Studies of Unmitigated and Mitigated Disruptions in ITER for Tungsten First Wall using TSC Simulations	Trivesh Kant
Study of Voltage Handling Capability of Hybrid Combiner for ITER Ion Cyclotron Radio Frequency Source	Akhil Jha

Acknowledgement

The HPC Team, Computer Division IPR, would like to thank all Contributors for the current issue of *GANANAM*.

Join the HPC Users Community

hpcusers@ipr.res.in

If you wish to contribute an article in *GANANAM*, please write to us.



Contact us

HPC Team
Computer Division, IPR
Email: hpcteam@ipr.res.in

Disclaimer: "*GANANAM*" is IPR's informal HPC Newsletter to disseminate technical HPC related work performed at IPR from time to time. Responsibility for the correctness of the Scientific Contents including the statements and cited resources lies solely with the Contributors.